

Journal of Visualized Experiments

Imaging dendritic spines in Caenorhabditis elegans

--Manuscript Draft--

Article Type:	Invited Methods Collection - JoVE Produced Video
Manuscript Number:	JoVE62676R2
Full Title:	Imaging dendritic spines in Caenorhabditis elegans
Corresponding Author:	David Miller Vanderbilt University Nashville, TN UNITED STATES
Corresponding Author's Institution:	Vanderbilt University
Corresponding Author E-Mail:	david.miller@vanderbilt.edu
Order of Authors:	Andrea Cuentas-Condori David Miller
Additional Information:	
Question	Response
Please specify the section of the submitted manuscript.	Neuroscience
Please indicate whether this article will be Standard Access or Open Access.	Open Access (\$3900)
Please indicate the city, state/province, and country where this article will be filmed . Please do not use abbreviations.	Nashville, TN, USA
Please confirm that you have read and agree to the terms and conditions of the author license agreement that applies below:	I agree to the Author License Agreement
Please provide any comments to the journal here.	
Please confirm that you have read and agree to the terms and conditions of the video release that applies below:	I agree to the Video Release

TITLE:

Imaging Dendritic Spines in *Caenorhabditis elegans*

AUTHORS AND AFFILIATIONS:

Andrea Cuentas-Condori¹, Miller D. M. III^{1,2*}

¹Department of Cell and Developmental Biology, Vanderbilt University, Nashville, TN, USA

²Program of Neuroscience, Vanderbilt University, Nashville, TN, USA

Email addresses of the authors:

Andrea Cuentas-Condori (andrea.a.cuentas.condori@vanderbilt.edu)

Miller DM III (david.miller@vanderbilt.edu)

*Email address of the corresponding author:

Miller DM III (david.miller@vanderbilt.edu)

SUMMARY:

Dendritic spines are important cellular features of the nervous system. Here live imaging methods are described for assessing the structure and function of dendritic spines in *C. elegans*. These approaches support the development of mutant screens for genes that define dendritic spine shape or function.

ABSTRACT:

Dendritic spines are specialized sites of synaptic innervation modulated by activity and serve as substrates for learning and memory. Recently, dendritic spines have been described for DD GABAergic neurons as the input sites from presynaptic cholinergic neurons in the motor circuit of *Caenorhabditis elegans*. This synaptic circuit can now serve as a powerful new *in vivo* model of spine morphogenesis and function that exploits the facile genetics and ready accessibility of *C. elegans* to live-cell imaging.

This protocol describes experimental strategies for assessing DD spine structure and function. In this approach, a super-resolution imaging strategy is used to visualize the intricate shapes of actin-rich dendritic spines. To evaluate the DD spine function, the light-activated opsin, Chrimson, stimulates the presynaptic cholinergic neurons, and the calcium indicator, GCaMP, reports the evoked calcium transients in postsynaptic DD spines. Together, these methods comprise powerful approaches for identifying genetic determinants of dendritic spines in *C. elegans* that could also direct spine morphogenesis and function in the brain.

INTRODUCTION:

Dendritic spines are specialized cellular structures that receive input from neighboring neurons for synaptic transmission. Activation of neurotransmitter receptors elevates intracellular calcium and downstream signaling pathways in this characteristic neuronal protrusions¹. Because of the fundamental importance of dendritic spines to neurotransmission and their misregulation in neurodevelopmental diseases¹, the discovery of factors that modulate dendritic spine

morphogenesis and function is of high interest to the field of neuroscience.

Recently, dendritic spines have been identified in the *C. elegans* nervous system based on key characteristics shared with mammalian spines². This determination is crucial because it opens the possibility of exploiting the advantages of *C. elegans* to investigate spine biology. Dendritic spines on Dorsal D (DD) motor neurons receive input from cholinergic neurons (VA and VB) in the ventral nerve cord (**Figure 1A**)²⁻⁴. Here, imaging methods are presented to explore the structure of DD dendritic spines and their function *in vivo* in an intact nervous system that is readily accessible to live imaging and genetic analysis. For monitoring the shape of dendritic spines, (1) cytosolic fluorescent proteins, which fill the dendritic process and spines; (2) membrane-bound fluorescent proteins, which decorate the border of dendritic spines and dendrites; or (3) the actin markers, LifeAct⁵ or Utrophin⁶, which are enriched in dendritic spines are used, thus revealing their shape. To monitor the functionality of DD spines, record Ca⁺⁺ transients with GCaMP and activate the presynaptic cholinergic neuron with the red-shifted opsin, Chrimson⁷. Both strategies are expected to facilitate the study of DD dendritic spines in wild-type and mutant animals.

PROTOCOL:

1. Determination of the structure of the DD dendritic spines

1.1. Create transgenic worms to label DD spines

1.1.1. Use the *flp-13* promoter to build an expression vector for the label of interest (e.g., cytoplasmic mCherry, MYR::mRuby, LifeAct::GFP, GFP::utrophin) (**Figure 1**). See the complete list of plasmids in **Supplementary File 1**.

1.1.2. Use established methods to generate a transgenic line labeling DD spines^{8,9}.

1.2. Prepare the sealant

1.2.1. Make a 1:1 mixture of paraffin-based embedding medium¹⁰ (see **Table of Materials**).

1.2.2. Heat the medium at 60 °C until melting, then aliquot in 1.5 mL capped microcentrifuge tubes and maintain a heating block at 60-70 °C.

NOTE: Sealant can last for 4 weeks in the heating block.

1.3. Prepare an anesthetic.

1.3.1. Make stock solutions in distilled H₂O of 1% Tricaine and 1 M levamisole (see **Table of Materials**). Store at -20 °C.

1.3.2. Prepare a working solution of 0.05% Tricaine and 15 mM levamisole anesthetic, as described in steps 1.3.3-1.3.5¹¹.

1.3.3. Mix 75 μ L of 1% Tricaine stock and 22.5 μ L of 1 M levamisole.

1.3.4. Add M9 buffer to a final volume of 1.5 mL.

1.3.5. Aliquot 10 μ L of 0.05% Tricaine, 15 mM levamisole into 0.5 mL microcentrifuge tubes and store at -20 °C.

NOTE: The anesthetic mixture is sensitive to temperature, and individual aliquots of the working solution should not be refrozen after thawing for each experiment. See **Supplementary File 2** for a recipe for M9 buffer.

1.4. Acquire high-resolution images

1.4.1. Prepare 10% agarose and maintain it in the water bath at 60 °C.

NOTE: See the report by Monica Driscoll in WormBook¹².

1.4.2. Mount 15-20 young adults on 10% agarose pads and add 3 μ L of anesthetic (see step 3).

1.4.3. Apply coverslip (worms are immobilized within 5 min).

1.4.4. Seal the edges of the coverslip with melted adhesive sealant mixture (see **Table of Materials**).

1.4.5. Acquire images

1.4.5.1. Super-resolution acquisition

1.4.5.1.1. Use a laser-scanning confocal microscope equipped for super-resolution microscopy with a 63x/1.40 Plan-Apochromat oil objective lens to achieve a small pixel size (e.g., < 50 nm). Acquire Z-stacks using the step size recommended by the manufacturer's software (see **Table of Materials**).

1.4.5.1.2. Collect a series of optical sections that span the total volume of the DD ventral process (e.g., 15–20 slices at 0.19 μ m step size or 2– 3 μ m thick). Submit Z-stacks for image processing using the manufacturer's software and analyze images with a score higher than 7 (**Figure 1B**, **Figure 2** and **Figure 3**).

1.4.5.2. Nyquist acquisition

1.4.5.2.1. Use a laser scanning confocal microscope to select the optimal pixel size for the wavelength of light and numerical aperture of the objective lens in use (e. g., 40x/1.4 Plan Fluor oil objective).

NOTE: The smaller pixel size will reveal the fine structure of DD spines.

1.4.5.2.2. Submit stack for 3D deconvolution using Automatic algorithm (see **Table of Materials**) (**Figure 3**).

1.4.5.3. Use the smallest Z-step possible (e.g., determined by Piezo stage) because oversampling in Z can yield sharper images after 3D deconvolution¹³.

1.5. Image analysis

1.5.1. Use an appropriate image processing software (see **Table of Materials**) to create maximum intensity projections of the Z-stacks¹⁴.

1.5.2. Manually count the protrusions on the DD dendrite.

NOTE: Protrusions are perpendicular extensions from the main shaft (**Figure 1B**, arrowheads).

1.5.3. Determine the length of the DD dendrite scored to calculate the density of spines per 10 μm of DD dendrite (**Figure 1C**).

1.5.4. Classify spines as thin/mushroom, filopodial, stubby or branched (**Figure 2A**).

NOTE: Thin/mushroom spines exhibit a narrow base (neck) and a broader tip (head). Filopodial spines do not display a constricted base (no neck) but have a constant width. Stubby spines have a wide base and tip. Branched spines are protrusions with more than one tip.

2. Assessing activation of DD dendritic spines by presynaptic cholinergic signaling

2.1. Create transgenic worms using conventional techniques (e.g., microinjection)^{8,9}

2.1.1. Use the *flp-13* promoter to drive expression of the Ca^{++} sensor, GCaMP6s, in DD neurons and the *unc-4* promoter to drive expression of Chrimson, a red-shifted channelrhodopsin, in presynaptic VA neurons (**Figure 4A**). See the list of plasmids in **Supplementary File 1**.

2.2. Prepare All-trans Retinal (ATR) and control plates.

NOTE: ATR is a required cofactor for Chrimson to function as an optogenetically activated ion channel.

2.2.1. Prepare 100 mM ATR stock solution in ethanol (100%). Store at $-20\text{ }^{\circ}\text{C}$ in 1 mL aliquots.

2.2.2. Under a laminar flow hood, add 300 μL of overnight OP50 bacterial culture and 0.25 μL of ATR to each 60 mm NGM (Nematode Growth Medium) nutrient agar plate and spread with a sterile glass rod.

2.2.3. For controls, add 300 μL of OP50 bacteria and 0.25 μL of ethanol (100%) to a separate group of NGM plates.

2.2.4. Let plates sit in hood at room temperature for 24 h (protected from ambient light) to allow bacterial growth.

NOTE: Plates can be used after the initial 24 h incubation or maintained at 4 °C to use within 5 days.

2.3. Setting-up the experiment

2.3.1. Place five NC3569 L4-stage larvae on OP50-seeded ATR or control plates that lack ATR and grow in darkness at 23°C.

2.3.2. Three days later, use a stereo dissecting microscope to confirm vulva development to pick L4 stage progeny from ATR and control plates for imaging as described in steps 2.4.1-2.4.3.

2.3.3. On a microscope slide, place 2 μL of 0.05 μm polybeads (2.5% solids w/v) (see **Table of Materials**).

2.3.4. Use a platinum wire (“worm pick”) to add a small globule of super glue to the solution and swirl gently to generate filamentous “strands” of glue. Then add 3 μL of M9 buffer (**Figure 4B**).

2.3.5. Place approximately ten L4 larvae in the solution and apply a coverslip.

NOTE: Glue fibers will randomly contact worms and immobilize them after the coverslip is applied. Worms that are embedded in large globules of glue appear desiccated and should not be imaged.

2.3.6. Seal edges of coverslip as mentioned in step 1.4.4.

2.4. Recording of the evoked Ca^{++} transients in dendritic spines.

2.4.1. Use a spinning disk confocal microscope equipped with a sensitive CCD camera, a 100x TIRF oil objective lens, and 488 nm and 561 nm laser lines (see **Table of Materials**).

2.4.2. Adjust microscope stage to position DD spines in the focal plane.

2.4.3. Set-up time-lapse acquisition to illuminate the sample with 488 nm laser line every frame (for detecting GCaMP6s fluorescence) and the 561 nm laser line at periodic intervals (for Chrimson excitation).

NOTE: For example, use 488 nm light to capture consecutive snapshots (200 ms) of GCaMP6s signal coupled with a 200 ms pulse of 561 nm light every 5th frame (**Figure 4C-E**). With this configuration, GCaMP levels before and after each 561 nm pulse are detected ~1 s apart (200 ms of 488 nm laser to detect GCaMP before VA activation, 200 ms of 561 nm pulse to activate VA and ~600 ms to switch between laser lines and emission filters. With this set-up, VA neurons are activated every 2.5 s.

2.5. Analysis of *in vivo* Ca⁺⁺ imaging

2.5.1. Use 2D-deconvolution and image alignment to correct minor deviations from the worm movement during acquisition (see **Table of Materials**).

2.5.2. Define the DD dendritic spine as the Region Of Interest (ROI in **Figures 4C-D**).

2.5.3. Duplicate the ROI and relocate to a neighboring region inside the worm to collect background signal (i.e., noise).

2.5.4. Use appropriate software (see **Table of Materials**) to export GFP intensities to excel for each time point. Subtract background fluorescence from spine ROI fluorescence.

2.5.5. Determine the change in fluorescence by subtracting the GFP fluorescence in the frame immediately before 561 nm excitation (F₀) from each time-point after excitation (ΔF), then dividing by F₀ to determine $\Delta F/F_0$ (**Figure 4E**).

2.5.6. Graph the normalized traces (See **Table of Materials**).

2.5.7. Perform a paired statistical test for each measurement of GCaMP6s fluorescence before and after each pulse of 561 nm light.

NOTE: This approach effectively excludes random fluctuations in GCaMP6s fluorescence that otherwise reduce the statistical power of comparing the mean GCaMP6s signal from all measurements before and after 561 nm excitation (**Figure 4F**).

2.5.8. For measurements that show a normal or Gaussian distribution, use a paired parametric ANOVA test and correct for multiple comparisons for each of the two groups (ATR before vs. after, no ATR before vs. after). Alternatively, for data that are not normally distributed, use a non-parametric ANOVA with posthoc correction for multiple testing.

NOTE: Worms grown on plates that lack ATR (“no ATR”) are necessary controls and should not show 561 nm-activated Ca⁺⁺ transients because ATR is required for Chrimson function.

REPRESENTATIVE RESULTS:

Measurements with three independent markers (cytosolic mCherry, LifeAct::GFP, MYR::mRuby) yielded an average density of 3.4 ± 1.03 DD dendritic spines per 10 μ m of DD dendrite in wild-

type young adults (**Figure 1B,C**). For this analysis, the measurements obtained with the GFP::Utrophin marker that yielded a significantly lower spine density were excluded (2.4 ± 0.74 , **Figure 1**) potentially due to interactions of Utrophin with the actin cytoskeleton⁶ that drives spine morphogenesis¹⁵. The measurements of spine density in the light microscope are comparable to the value of 4.2 spines/10 μm dendrite obtained from the reconstruction of 12 spines from electron micrographs of the DD1 neuron². The live-cell imaging approach confirmed that the thin/mushroom-shaped morphology of the DD spines predominates in the adult vs. alternative spine shapes (e.g., filopodial, stubby, branched) (**Figure 2B**), which is also typical for spines in the mature mammalian nervous system¹⁶.

An optogenetic strategy was used to ask if the presumptive dendritic spines detected by high-resolution light microscopy (**Figure 1** and **Figure 2**) are responsive to neurotransmitter release from presynaptic sites, a characteristic hallmark of dendritic spines in mammalian neurons. Greenlight (561 nm) was used to activate a channelrhodopsin variant, Chrimson, in presynaptic cholinergic neurons and blue light (488 nm) to detect Ca^{++} -dependent fluorescence emitted by a cytoplasmic GCaMP probe in postsynaptic DD dendritic spines. This experiment detected transient bursts of GCaMP signal in DD spines immediately after optogenetic activation of Chrimson in presynaptic VA neurons (**Figure 3**). The success of this experiment depends on the reliable expression of Chrimson in all presynaptic VA neurons. In this case, a chromosomal integrant of the *Punc-4::Chrimson* marker was used to ensure consistent VA expression¹⁷. This experiment could also be conducted with an extrachromosomal array. Chrimson expression in a specific VA neuron can be independently confirmed, for example, by coupling the Chrimson transgene to an SL2 transplanted leader sequence with a downstream nuclear-localized GFP as a co-expression marker². It is essential to perform a control experiment in the absence of ATR to confirm that the measured GCaMP signal depends on optogenetic activation of Chrimson, which is strictly ATR-dependent (**Figure 4D**). Finally, because evoked Ca^{++} signals are transient, it is crucial to adopt an imaging protocol that allows rapid switching (<1 s) between 561 nm excitation and GCaMP signal acquisition with the 488 nm laser (**Figure 4**).

FIGURE LEGENDS:

Figure 1: Labeling of DD dendritic spines. (A) (Top) Six Dorsal D (DD1-DD6) neurons in the ventral nerve cord of *C. elegans*. (Bottom) In adults, ventrally directed DD spines (arrowhead) contact presynaptic terminals of Ventral A (VA) and Ventral B (VB) motor neurons (magenta), and DD commissures extend to the dorsal nerve cord to provide GABAergic output to body muscles (arrow)¹⁸. This figure has been modified from Reference². (B) Fluorescent micrographs (Airyscan) of DD spines labeled with cytosolic mCherry, myristoylated mRuby (MYR::mRuby), LifeAct::GFP and GFP::Utrophin in young adult worms. Gray arrowheads point to spines. Scale bar = 2 μm . (C) Density (spines/10 μm) of DD neuron dendritic spines labeled with cytosolic mCherry (3.77 ± 0.9), MYR::mRuby (3.09 ± 0.8), LifeAct::GFP (3.44 ± 1.1) or GFP::Utrophin (2.41 ± 0.8). All samples are normally distributed. One-Way ANOVA shows that spine densities for cytosolic mCherry, MYR::mRuby, and LifeAct::GFP are not significantly (NS) different, whereas spine density is reduced for GFP::Utrophin vs. cytosolically labeled mCherry ($p = 0.0016$) and LifeAct::GFP ($p = 0.0082$). The dashed red line represents the spine density of DD neurons assessed from 3D EM

reconstruction (4.2 spines/10 μ m). This figure has been modified from Reference².

Figure 2: Imaging DD dendritic spines. (A) (Top) Schematic of spine shapes. (Bottom) Airyscan images of each type of spine (Scale bar = 500 nm) labeled with LifeAct::GFP (green) and 3D-reconstructions by serial electron micrographs of a high-pressure frozen adult (blue). (B) Spine frequency by type, visualized with LifeAct::GFP: Thin/Mushroom ($55.5 \pm 14.5\%$), Filopodial ($10.3 \pm 8.70\%$), Stubby ($18.8 \pm 10.7\%$), Branched ($15.42 \pm 6.01\%$). Spines frequency by type visualized with MYR::mRuby: Thin/Mushroom ($52.2 \pm 16.5\%$), Filopodial ($5.68 \pm 7.0\%$), Stubby ($33.1 \pm 14.8\%$), Branched ($9.02 \pm 9.6\%$). Unpaired T-test, Filopodial ($p = 0.0339$); Stubby ($p = 0.0009$) and Branched ($p = 0.011$) spines labeled with the MYR::mRuby marker are significantly different from LifeAct::GFP. This figure has been modified from Reference².

Figure 3: Strategies for acquiring high-resolution images of DD spines. (A-B) (Top) Fluorescent images of DD1 dendrites labeled with a cytosolic marker (mCherry) by (A) Airyscan detector and (B) Nyquist acquisition. (Bottom) DD dendrite (red) is depicted with an image analysis software (auto-path option of filament tracer), and DD spines (blue) are graphically illustrated using the semi-automated spines detection module. Arrow points to branched spine enlarged in C and D. Arrowheads denote neighboring thin/mushroom spines enlarged in C and D. Scale bar = 2 μ m. (C-D) Enlarged examples of (top) branched spine (arrow) and (bottom) two neighboring thin/mushroom spines (arrowheads) obtained with (C) Airyscan detector or by (D) Nyquist acquisition. Scale bar = 500 nm. Data reproduced from².

Figure 4: Assessing the function of DD spines. (A) DD motor neurons express the Ca^{++} indicator GCaMP6s (green), and VA motor neurons express the channelrhodopsin-variant, Chrimson (magenta)⁷. (B) Schematic depicting method for mounting worms for Ca^{++} measurements. (1) On a clean microscope slide, (2) place 2 μ L of 0.05 μ m poly beads, (3) use a platinum wire ("worm pick") to add a small globule of super glue and (4) swirl into the solution to generate filamentous strands of glue. (5) Add 3 μ L of M9 buffer. (6) Place approximately ten L4 larvae in the solution, (7) apply coverslip and seal edges with Vaseline/wax. (C-D) Activation of VA neurons correlates with Ca^{++} transients in DD1 spines. GCaMP6s fluorescence imaged (at 0.5 s intervals) with periodic light activation of Chrimson (2.5 s intervals) evokes Ca^{++} transients with (C) +ATR ($n = 12$) but not in (D) controls (-ATR, $n = 12$). Panels are snapshots over time (s), before and after pulse of 561 nm light (vertical pink line). Scale bars = 2 μ m. GCaMP6s signal is acquired from an ROI (Region of Interest) at the tip of each spine. (E) GCaMP6s fluorescence during the 10 s recording period plotted for +ATR (green) vs -ATR (control, gray) ($n = 12$ videos). Vertical pink bars denote 561 nm illumination (e.g., Chrimson activation). Each animal was stimulated 4 times with 561 nm light. Measurements were collected before and after each pulse of 561 nm light. (F) Plot of the GCaMP6s fluorescence before and after each pulse of 561 nm light. GCaMP6s fluorescence was measured 1 s after each pulse of 561 nm light. Because samples are not normally distributed, a paired non-parametric Friedman test was applied to correct for multiple comparisons of GCaMP6s fluorescence before vs. after 561 nm light stimulation for worms grown either with ATR (+ATR, green) (** $p = 0.0004$, $n = 48$ measurements) or in the absence of ATR (-ATR, gray) (NS, Not Significant, $p = 0.0962$, $n = 48$ measurements). This figure has been modified from Reference².

Supplementary File 1: List of plasmids used in the study.

Supplementary File 2: Composition and preparation of M9 buffer.

DISCUSSION:

The Airyscan detector was selected to acquire snapshots of DD spines because it affords a higher signal-to-noise ratio and better resolution than conventional confocal microscopes^{19,20}. AiryScan imaging also allows the use of conventional fluorescent proteins (e.g., GFP, mCherry, etc.), now widely available for *C. elegans*. Although higher resolution images can be obtained with other super-resolution methods (e.g., STORM, STED, PALM), these methods require photo-activatable or photo-switchable fluorescent proteins²¹. As an alternative to Airyscan, conventional confocal microscopes are recommended. For example, imaging with Nyquist acquisition (**Figure 3**) achieves the pixel size using a 40x/1.3 objective of 123.9 nm, sufficient to distinguish the spine morphological types (**Figure 2**).

For determining spine density, using a cytosolic fluorescent protein such as (1) mCherry or GFP, (2) LifeAct to label the actin cytoskeleton, or (3) a myristoylated fluorescent protein (e.g., MYR::mRuby) to label the plasma membrane (**Figure 1B**) is recommended. In comparison, the F-actin binding protein Utrophin reduces spine density (**Figure 1C**), indicating a negative effect on spine morphogenesis when Utrophin is over-expressed.

The current imaging methods should help identify genetic variants that govern spine morphology^{1,16}. DD spine morphology (i.e., thin/mushroom, filopodial, stubby, branched, see **Figure 2**) can be assessed from single 2D-projections of the ventral nerve cord lateral images since most DD spines adopt a characteristically ventrally-directed orientation. In these comparisons, it is essential to use the same fluorescent marker for each condition since apparent spine morphological types seem to be influenced by the labeling method (e.g., MYR::mRuby vs. LifeAct::GFP). In addition, it was noted that the spine shapes are dynamic and likely change shape in response to the external signals^{2,16}. Thus, it is also essential to compare spine shapes between genotypes at similar developmental stages and under similar conditions.

The orientation of the *C. elegans* ventral cord is critically vital for accurate image acquisition. Both the ventral and dorsal cords on opposite sides of the animal should be visible in the same Z-plane, indicating that the worm is oriented on its side (**Figure 1B**). It is best not to collect images of worms moving or in contact with other worms or bubbles near the ventral cord, as this can degrade images of spines.

For *in vivo* calcium imaging, fresh slides need to be prepared immediately before each acquisition. It is best to image worms in contact with only thin glue fibers vs. “globs” of glue which tend to desiccate worms and degrade the image (**Figure 4B**). In the experiment shown in **Figure 4**, the pulse of 561 nm light activates the entire field of view. For increasing the temporal and spatial resolution to detect local Ca⁺⁺ transients, for example, within individual DD spines, a galvo mini scanner set up for the 561 nm laser line can be used to stimulate a smaller region of

interest¹⁷.

ACKNOWLEDGMENTS:

Imaging and analysis on Imaris were performed in the Vanderbilt Cell Imaging Shared Resource (CIRS) supported by NIH (CA68485, DK20593, DK58404, DK59637, and EY08126). The LSM 880 is supported by grant 1S10OD201630. Imaging on a Nikon spinning disk was performed at the Nikon Center of Excellence. We thank Jenny Schafer, CIRS director, and Bryan Millis for training and insightful discussions and members of the Burnette lab: Dylan Burnette, Aidan Fenix, and Nilay Taneja for advice. This work was supported by National Institutes of Health grants to DMM (R01NS081259 and R01NS106951) and an American Heart Association grant to ACC (18PRE33960581).

DISCLOSURES:

We declare no conflicts of interest.

REFERENCES:

1. Sala, C., Segal, M. Dendritic Spines: The Locus of Structural and Functional Plasticity. *Physiological Reviews*. **94** (1), 141–188 (2014).
2. Cuentas-Condori, A. et al. C. elegans neurons have functional dendritic spines. *Elife*. **8**, e47918 (2019).
3. Philbrook, A. et al. Neurexin directs partner-specific synaptic connectivity in C. Elegans. *Elife*. **7**, e35692 (2018).
4. Oliver, D., Alexander, K., Francis, M. M. Molecular Mechanisms Directing Spine Outgrowth and Synaptic Partner Selection in Caenorhabditis elegans. *Journal of Experimental Neuroscience*. **12**, 10–13 (2018).
5. Riedl, J. et al. Lifeact: a versatile marker to visualize F-actin. *Nature Methods*. **5**, 605–607 (2008).
6. Ladt, K., Ganguly, A., Roy, S. Axonal actin in action: Imaging actin dynamics in neurons. *Methods of Cell Biology*. **131**, 91–106 (2016).
7. Schild, L. C., Glauser, D. A. Dual color neural activation and behavior control with chrimson and CoChR in Caenorhabditis elegans. *Genetics* **200** (4), 1029–1034 (2015).
8. Mello, C., Kramer, J., Stinchcomb, D., Ambros, V. Efficient gene transfer in C. elegans: extrachromosomal maintenance and integration of transforming sequences. *The EMBO Journal*. **10** (12), 3959–3970 (1991).
9. Berkowitz, L. A., Knight, A. L., Caldwell, G. A., Caldwell, K. A. Generation of Stable Transgenic C. elegans Using Microinjection. *Journal of Visualized Experiments*. **18**, e833 (2008).
10. Smith, C. J. et al. Time-lapse imaging and cell-specific expression profiling reveal dynamic branching and molecular determinants of a multi-dendritic nociceptor in C. elegans. *Developmental Biology*. **345** (1), 18–33 (2010).
11. McCarter, J., Bartlett, B., Dang, T., Schedl, T. Soma – Germ Cell Interactions in Caenorhabditis elegans : Multiple Events of Hermaphrodite Germline Development Require the Somatic Sheath and Spermathecal Lineages. *Developmental Biology*. **181** (2), 121–143 (1997).
12. Driscoll, M. Mounting animals for observation with Nomarski DIC optics. *WormBook* (2008).

- 441 13. North, A. J. Seeing is believing? A beginners' guide to practical pitfalls in image acquisition.
442 *Journal of Cell Biology*. **172** (1), 9–18 (2006).
- 443 14. Schindelin, J. et al. Fiji: An open-source platform for biological-image analysis. *Nature*
444 *Methods*. **9**, 676–682 (2012).
- 445 15. Hotulainen, P. & Hoogenraad, C. C. Actin in dendritic spines : connecting dynamics to
446 function. *Journal of Cell Biology*. **189** (4), 619–629 (2010).
- 447 16. Berry, K. P., Nedivi, E. Spine Dynamics: Are They All the Same? *Neuron*. **96** (1), 43–55
448 (2017).
- 449 17. Miller, D. M., Niemeyer, C. J. Expression of the unc-4 homeoprotein in *Caenorhabditis*
450 *elegans* motor neurons specifies presynaptic input. *Development*. **121** (9), 2877–2886 (1995).
- 451 18. White, J. G., Southgate, E., Thomson, J. N., Brenner, S. The Structure of the Ventral Nerve
452 Cord of *Caenorhabditis elegans*. *Philosophical Transactions of the Royal Society*. **275** (938), 327-
453 348 (1976).
- 454 19. Huff, J. The Airyscan detector from ZEISS : confocal imaging with improved signal-to-noise
455 ratio and super-resolution. *Nature Methods*. **12**, i-ii (2015).
- 456 20. Huff, J. The Fast mode for ZEISS LSM 880 with Airyscan : high-speed confocal imaging with
457 super-resolution and improved signal-to-noise ratio. *Nature Methods*. **13**, i-ii (2016).
- 458 21. Jacquemet, G., Carisey, A. F., Hamidi, H., Henriques, R., Leterrier, C. The cell biologist's
459 guide to super-resolution microscopy. *Journal of Cell Science*. **133** (11) jcs240713 (2020).
- 460

Figure 1 - Labeling DD dendritic spines

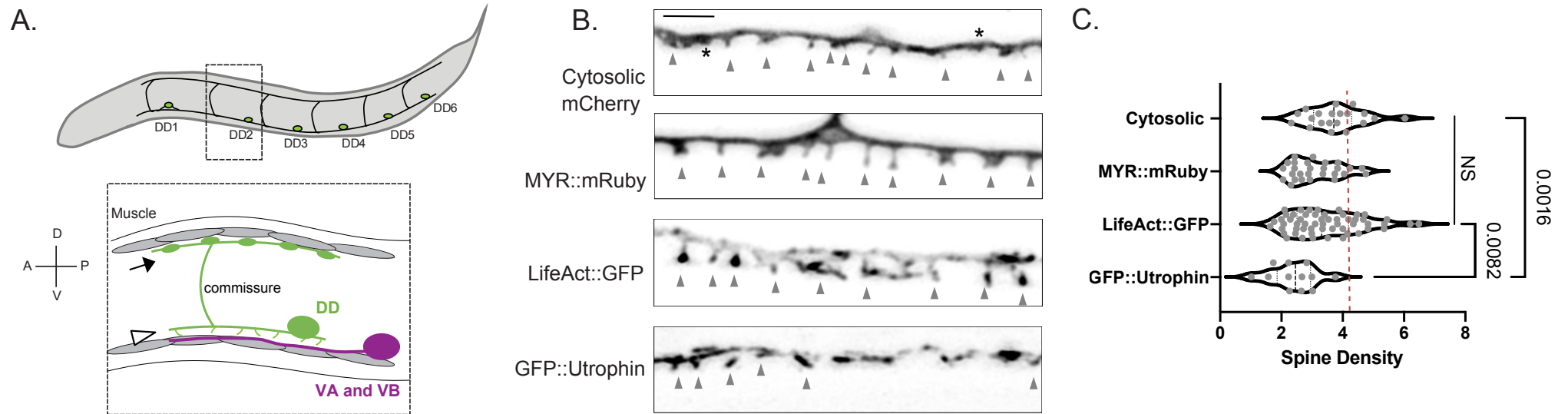


Figure 2 - Determining the shape of DD dendritic spines

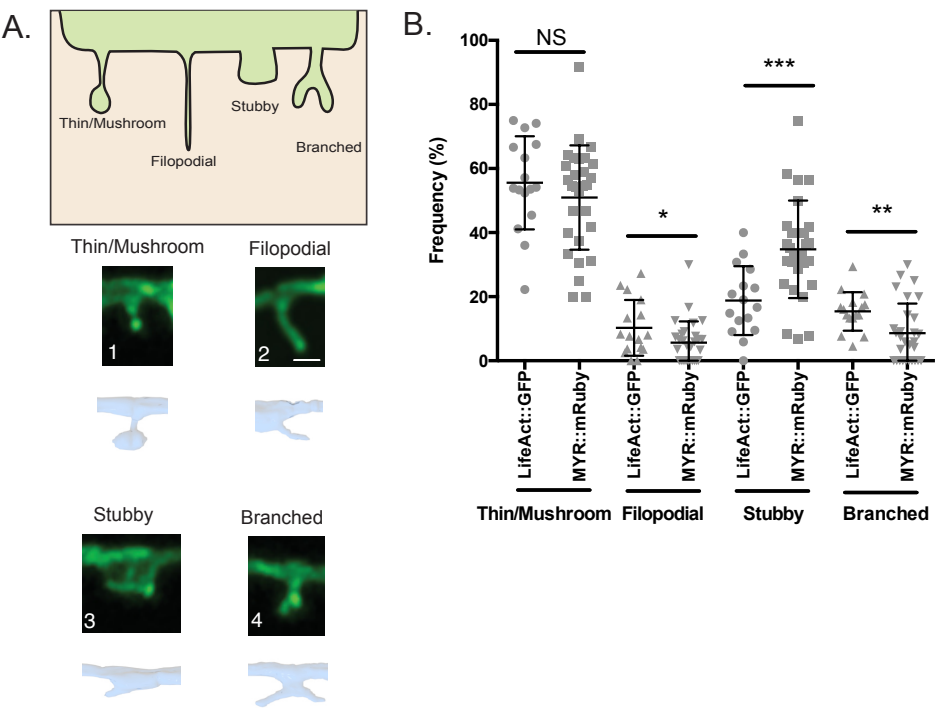


Figure 3 - Alternative systems to image DD spines

A. Airyscan detector

B. Nyquist acquisition

pixel size: 49.0 nm

pixel size: 123.9 nm

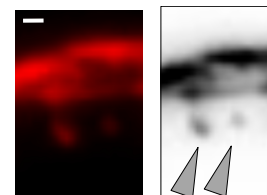
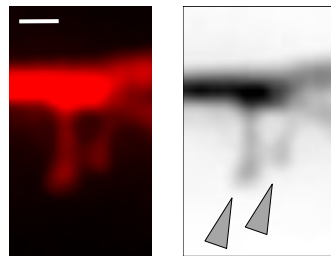
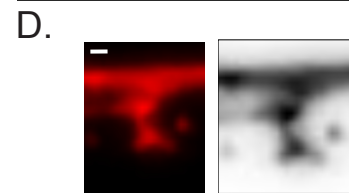
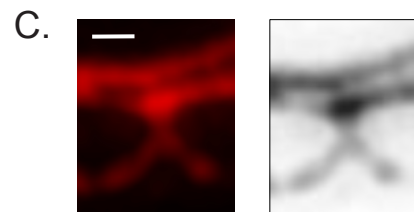
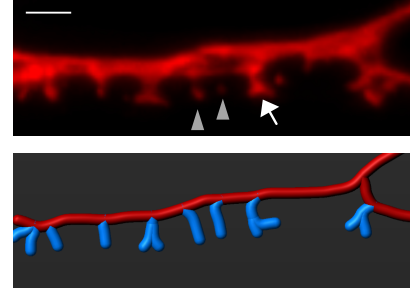
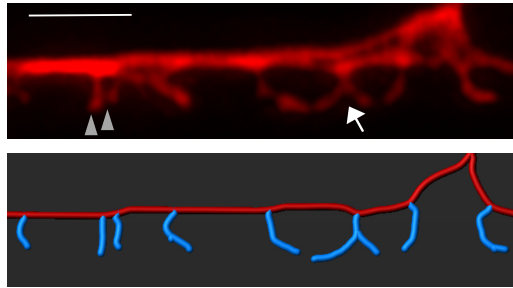
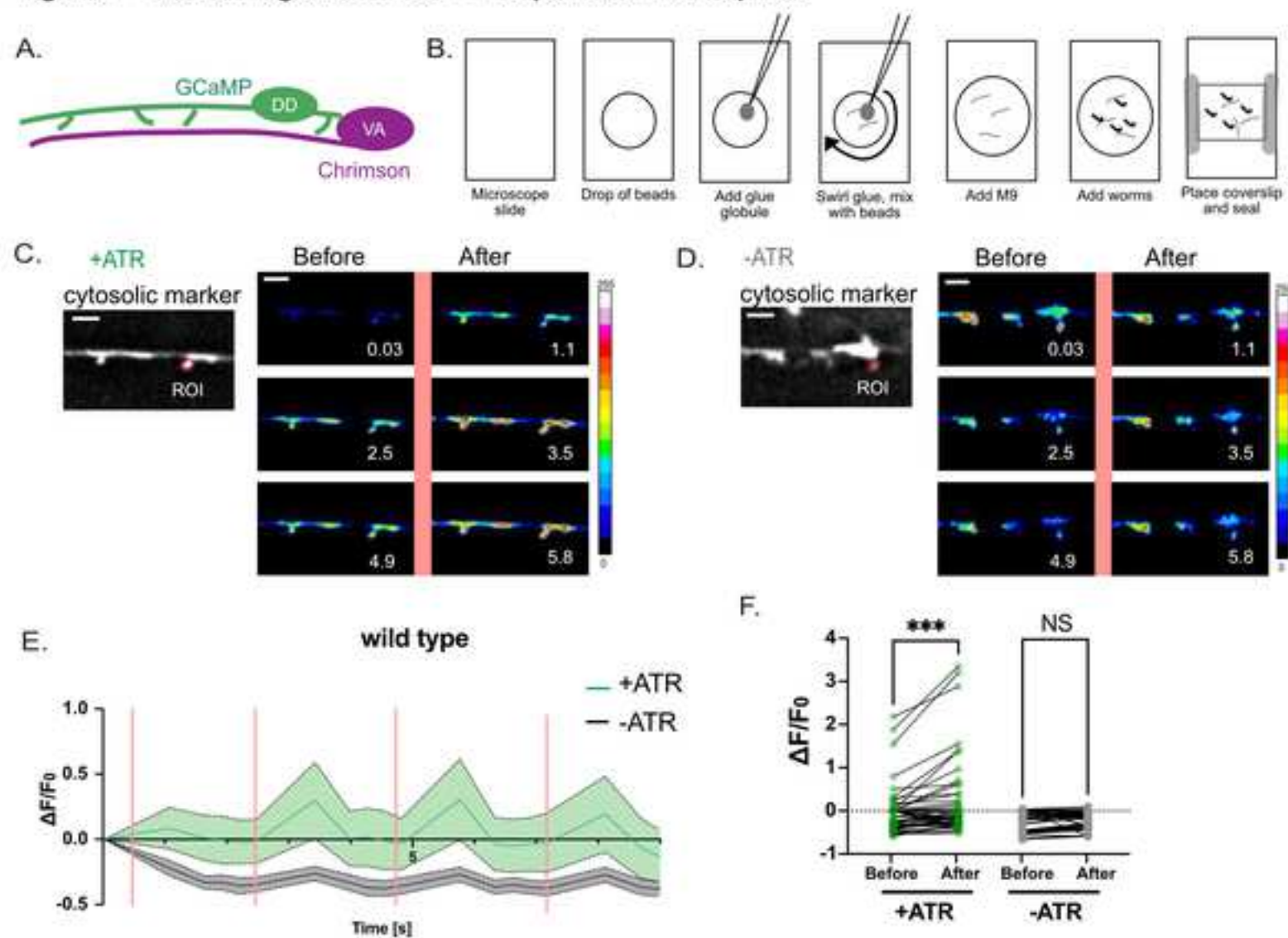


Figure 4 - Measuring evoked Ca^{++} responses in DD spines



Click here to access/download

Table of Materials
62676_R2_Table of Materials.xls



Editorial comments:

Changes to be made by the Author(s):

1. Please take this opportunity to thoroughly proofread the manuscript to ensure that there are no spelling or grammar issues. Please define all abbreviations at first use.

2. Please revise the following lines to avoid overlap with previously published work: 103-107 (if this is a note and not a step written in imperative tense); 239-243; 267-269;

Done.

3. Please provide an email address for each author.

andrea.a.cuentas.condori@vanderbilt.edu and david.miller@vanderbilt.edu

4. For in-text formatting, corresponding reference numbers should appear as numbered superscripts after the appropriate statement(s), but before punctuation.

We have updated references to the requested format.

5. JoVE cannot publish manuscripts containing commercial language. This includes trademark symbols (™), registered symbols (®), and company names before an instrument or reagent. Please remove all commercial language from your manuscript and use generic terms instead. All commercial products should be sufficiently referenced in the Table of Materials and Reagents.

For example: Zeiss Airyscan; Leica paraplast tissue embedding medium; Zeiss LSM880 microscope; Plan-Apochromat oil objective lens; AiryScan image processing using ZEN software; A1R Nikon microscope with Nyquist acquisition; NIS Elements, using Automatic algorithm; Polysciences, Inc. #15913-10; Yokogawa CSU-X1 spinning disk head, Andor DU-897 EMCCD camera, 100X/1.49 Apo TIRF oil objective lens and 488 nm and 561 nm laser lines; Super Glue, The Gorilla Glue Company etc.

We have modified the text accordingly.

6. Please revise the text, especially in the protocol, to avoid the use of any personal pronouns (e.g., "we", "you", "our" etc.).

We have eliminated all personal pronouns from the protocol section and have reduced their use in other sections of the manuscript.

7. Please ensure that all text in the protocol section is written in the imperative tense as if telling someone how to do the technique (e.g., “Do this,” “Ensure that,” etc.). The actions should be described in the imperative tense in complete sentences wherever possible. Avoid usage of phrases such as “could be,” “should be,” and “would be” throughout the Protocol. Any text that cannot be written in the imperative tense may be added as a “Note.” However, notes should be concise and used sparingly. Please include all safety procedures and use of hoods, etc.

We have removed all “could be,” “should be,” and “would be” from the protocol section.

8. Please note that your protocol will be used to generate the script for the video and must contain everything that you would like shown in the video. Please add more details to your protocol steps. Please ensure you answer the “how” question, i.e., how is the step performed? Alternatively, add references to published material specifying how to perform the protocol action. Please add more specific details (e.g., button clicks for software actions, numerical values for settings, etc) to your protocol steps. There should be enough detail in each step to supplement the actions seen in the video so that viewers can easily replicate the protocol.

These points are now addressed but we welcome additional input from the editor

9. After including a one-line space between each protocol step, highlight up to 3 pages of protocol text for inclusion in the protocol section of the video. This will clarify what needs to be filmed.

See highlighted text.

10. Convert this into a reference: See Mounting Animals for observation with Nomarski DIC protocol by Monica Driscoll in WormAtlas for guidance on how to prepare agarose pads (<https://www.wormatlas.org/agarpad.htm>).

We have added Monica Driscoll’s protocol as a reference.

11. Please ensure that the references appear as the following: [Lastname, F.I., LastName, F.I., LastName, F.I. Article Title. Source (ital). Volume (bold) (Issue), FirstPage–LastPage (YEAR).] For more than 6 authors, list only the first author then et al. Please include volume and issue numbers for all references, and do not abbreviate journal names.

References are now formatted as directed.

12. Please include a scale bar for all images taken with a microscope to provide context to the magnification used. Define the scale in the appropriate Figure Legend.

We have added scale bars to all microscopic images.

13. Please sort the Materials Table alphabetically by the name of the material.

Materials are now arranged alphabetically with the exception of microscopes which are listed together with associated components (e.g., objective lenses, laser lines, etc.).

Reviewers' comments:

Reviewer #1:

Manuscript Summary:

The authors give a comprehensive protocol for imaging dendritic spines in *C. elegans* based on their previous study (Cuentas-Condori et al., 2019). This protocol will be of use to multiple *C. elegans* researchers who are interested in imaging and studying dendritic spine morphology as well as signaling in dendritic spines using a calcium indicator in the DD spines. I support the publication of this protocol with minor changes that may improve the clarity of some points.

Major Concerns:

None

Minor Concerns:

Please find these concerns listed below:

A. Protocol:

1a: It is not clear if this is a promoter tag vs a translational fusion or either. Maybe the authors could elaborate by indicating the full plasmid as Pflp-13::MYR::mRuby etc.)

We have added a list of plasmids that details the promoters and protein products for each strategy that we used to label DD spines.

2. Note: Sealant can last for weeks (expand on approx. no. of weeks and also mention the temperature for storage).

We have specified that sealant can last at least for 4 weeks in a heating block at 60-70°C.

3. For stock solutions, it may help to say that they are made in ddH₂O or whichever solvent is used to make the solution. A reference to making M9 solution could be added to point no. 3d (recipe on page X would also be fine).

We now point readers to our supplementary information, which includes a recipe for M9 buffer.

4b: Approximate time required for immobilization could be added.

The revised protocol now states, "Apply coverslip (worms are immobilized within 5 minutes)."

B. Assessing activation of DD dendritic spines by presynaptic cholinergic signaling:

1a: Again, giving the entire plasmid as mentioned in 1a above would help the experimenter.

We have compiled the plasmid and strain names into a table that details the exact expression vectors and genotypes used.

2. ATR and NGM could be expanded here as this is the first instance for using these abbreviations.

Thanks, we now define the abbreviations, ATR and NGM.

2c ...to a separate group.....

Fixed.

2d It is not obvious in this point if one has to wait for 5 days or if using the plates immediately is fine too. This sentence could be reworded.

We have rephrased the sentence to indicate that plates can be used either immediately or within 5 days (See lines 142-143).

5a It may be useful to use Nikon NIS Elements instead of just NIS Elements.

Nikon NIS elements is now listed in the Table of Materials to conform with JoVE publishing guidelines.

Reviewer #2:

Manuscript Summary:

The goal of this paper and video is to describe how to assess structure of dendritic spines in the nematode *C. elegans*. The significance will be its utility in the characterization of mutants that may be defective for aspects of spine morphogenesis or synaptic function. The manuscript

describes reagents and the method for visualizing the dendritic spines of *C. elegans* using the LSM880 Zeiss AiryScan. The paper is well-written and includes beautiful images using the method. My comments are only for minor suggestions.

Broad Points:

(1) The authors state that the method can be used to define the function of dendritic spines but the paper only applies the method for morphological characterization of spine types. If the authors have such data, it would be good to include an example characterizing postsynaptic responses either at different synaptic types or in postsynaptic mutants.

The methods described in this article can be used to define spine function as well as structure. The calcium imaging methods that are featured here can be used to measure the response of spines to presynaptic cholinergic signaling and thus, in our view, satisfy our statement that methods described in our paper can be used to define spine function. Experiments that use these methods to measure postsynaptic responses at other synaptic types or in postsynaptic mutants are beyond the scope of this work.

(2) Probably the most important resource for the text portion of this JOVE publication is a strains and genotype table. We would like to know what we should order from the CGC. Some detail is important here. For example is the Punc-4::Chrimson integrant a single-copy insertion? Is it at the 5605 site on chromosome 2, which is becoming quite crowded these days? Or is it an integration of a multicopy array? If so, where?

Following the reviewer's suggestion, we have included a list of plasmids and strains and have deposited lines NC3315 and NC3569 with the CGC. The Punc-4::Chrimson::SL2::3xNLS::GFP integrant was produced by X-ray irradiation of a multicopy array. A reference is now included for this method (Miller and Niemeyer, 1995). The chromosomal location has not been determined.

Specific Points:

Line 63: The section about preparing stock solution is unclear. Distinction between tricaine and levamisole stocks, as well as 'working stock' of anesthetic, and final anesthetic concentrations needs to be made clear. The protocol closes with anesthetics are sensitive to temperature and should not be refrozen, but the protocol describes the stocks being frozen twice (they are separate at first – I understand that, but the language is unclear. Try out the protocol on an undergrad if you want to see where the confusion arises).

See line 76-77

Thank you for noting that this section is confusing. We have reworded this section to clarify (see lines 70-80).

Line 64: Is tricaine capitalized. I can't remember if it is a brand name or generic name.
Tricaine should be capitalized. Now corrected.

Line 112-113: Be consistent with promoter wormology. Once you mentioned "flp-13 promoter" and later you say "Punc-4 promoter".

Thank you for noting this discrepancy. It is now corrected.

Line 116: ATR is not defined. It might also be good to describe why retinal is required and what the 'no ATR' control is demonstrating.

We now define ATR (Lines 130-131). An explanation of the importance of the "no ATR" control is now provided (lines 199-201)

Line 134: Period instead of a comma.

Fixed.

Plasmids used in this study:

Plasmid Name	Description	Cloned by
Figure 1-3		
pACC6	Pflp-13::LifeAct::GFP	InFusion cloning
pACC100	Pflp13::GFP::Utrophin	InFusion cloning
pACC128	Pflp-13::myr::mRuby3	InFusion cloning
Figure 4		
pACC92	Punc-4::ceChrimson::SL2::3xNLS::GFP	InFusion cloning
pACC83	Pflp-13::GCaMP6s::SL2::mCherry	InFusion cloning

Strains used in this study:

Strain Name	Description	Reference
Figure 1-3		
XMN46	bglIs6 [Pflp-13::mCherry; PttX-3::RFP] II	(Opperman & Grill, 2014)
NC3315	wdEx1016 [Pflp-13::LifeAct::GFP; Pmyo-2::RFP]	(Cuentas-Condori et al., 2019)
NC3608	wdEx123[Pflp-13::myr::mRuby; Pstr-1::GFP]	(Cuentas-Condori et al., 2019)
NC3518	wdEx1108 [Pflp-13::GFP::Utrophin; Pmyo-2::RFP]	(Cuentas-Condori et al., 2019)
Figure 4		
NC3569	lin-15(n765); wdlIs117 [Punc-4::ceChrimson::SL2::3xNLSGFP; lin-15+] II?; wdEx1112 [Pflp13::GCaMP6s::SL2::mCherry]	(Cuentas-Condori et al., 2019)

Recipe:

M9 buffer (1 L Milli Q water)

KH_2PO_4 : 3 g

Na_2HPO_4 : 6 g

NaCl : 5 g

Autoclave at 121° C for 20 min.

1M MgSO_4 1 mL (add after autoclaving)

<https://reviewer.elifesciences.org/author-guide/journal-policies>

Licensing

Because articles published by eLife are licensed under a [Creative Commons Attribution license](#), others are free to copy, distribute, and reuse them (in part or in full), without needing to seek permission, as long as the author and original source are properly cited.